

## Asteroid (19) Fortuna: Triaxial Ellipsoid Dimensions and Rotational Pole with AO at Gemini North

J. Drummond (1), W. J. Merline (2), A. Conrad (3), J. Christou (4), P. Tamblyn (2), and B. Carry (5)

(1) Air Force Research Laboratory, Kirtland AFB, NM, USA, (2) Southwest Research Institute, Boulder, CO, USA, (3) Max Planck Institute for Astronomy, Heidelberg, Germany, (4) Gemini Observatory, Hilo, HI, USA, (5) European Space Astronomy Centre, Madrid, Spain

### ABSTRACT

The triaxial ellipsoid dimensions and rotational pole of the large asteroid (19) Fortuna were found from only three nights of adaptive optics images in November 2009 at the 8 meter Gemini North telescope at  $\lambda = 2.15\mu\text{m}$ . The dimensions and pole, as well as images, are supported by the model derived from lightcurve inversions [4] and stellar occultations. Fortuna should perhaps be considered a candidate for a Standard Triaxial Ellipsoid [2].

### Triaxial Ellipsoid Solution

In a continuing program to derive fundamental properties of asteroids with adaptive optics (AO), we observed the G-type asteroid (19) Fortuna over three nights in November 2009, at the Gemini North 8 m telescope. From its changing apparent elliptical size and orientation we derive its triaxial ellipsoid dimensions and locate its rotational pole to two possible regions, only one of which falls near poles derived from lightcurves. Table 1 contains ephemeris data for Fortuna for the middle night. At an image scale of  $0.022''/\text{pix}$  or  $46.8 \text{ km per resolution element}$  for the AO system at  $K'$  ( $2.15\mu\text{m}$ ) on Gemini North, Fortuna was well resolved. With the technique [1] of making a simultaneous fit in the Fourier plane for a Lorentzian point spread function and a flatly illuminated projected ellipse over the course of a few rotations, we derive the triaxial ellipsoid diameters and rotational pole given in Table 2 ( $\theta$  is sub-Earth latitude) and shown in Fig 1. Each rotational point is the mean result of measuring 12 consecutive images, three images at four places on the chip, for a total of 96 measured images over the three nights. All exposures were 0.5 seconds.

From the rotational poles [3] of asteroids as listed on a web site<sup>1</sup> of sidereal periods, rotational poles, and axial ratios, we plot the poles that fall near our accepted pole in Fig 2. Our other (rejected) pole lies

at  $[\lambda=49^\circ; \beta=-61^\circ]$ . The pole closest to ours is the Lightcurve Inversion (LCI) model<sup>2</sup> pole [4]  $6.5^\circ$  away.

Table 1. (19) Fortuna Observing Log (J2000)

UT Date	E Dist. (AU)	S Dist. (AU)	$V_{\text{mag}}$	Solar phase
2009 Nov 24	1.165	2.122	9.73	8.8°
	RA	Dec	Eclip. long	North to Sun
	80.6°	+21.3°	81.2°	-1.9° 91.8°

Table 2. (19) Fortuna Triaxial Ellipsoid Solutions

Parameter	This paper	LCI
Diam a (km)	$241 \pm 6$	249
Diam b (km)	$196 \pm 4$	206
Diam c (km)	$195 \pm 5$	198
$\theta$	$-26^\circ \pm 3$	$-30^\circ \pm 5$
Pole		
[RA; Dec]	$[145^\circ; +77^\circ]$	$[115^\circ; +80^\circ]$
$\sigma$ Radius	$5^\circ$	$5^\circ$
$[\lambda; \beta]$	$[110^\circ; +58^\circ]$	$[98^\circ; +57^\circ]$

For comparison, the results from our fitting the LCI model as a triaxial ellipsoid are also given in Table 2, along with its rotational pole. The LCI spherical equivalent diameter is listed<sup>2</sup> as  $210 \pm 12 \text{ km}$ , the same as our  $(abc)^{1/3}$ . Our errors in Table 2 are derived from our fit and an additional 2% possible systematic effect. Linearly deconvolved images are shown in Fig 3, and are compared to the LCI model at the same rotational phase. The agreement is gratifying.

### References

- 1 Conrad, A. R. et al: Icarus, 191, 616-627, 2007.
- 2 Drummond, J.D. et al.: BAAS 40, 427, 2008.
- 3 Kryszczyńska, A. et al.: Icarus, 192, 223-237, 2007.
- 4 Torppa J., et al.: Icarus 164, 346-383, 2003.

<sup>1</sup><http://vesta.astro.amu.edu.pl/Science/Asteroids/>

<sup>2</sup><http://astro.troja.mff.cuni.cz/projects/asteroids3D/web.php>

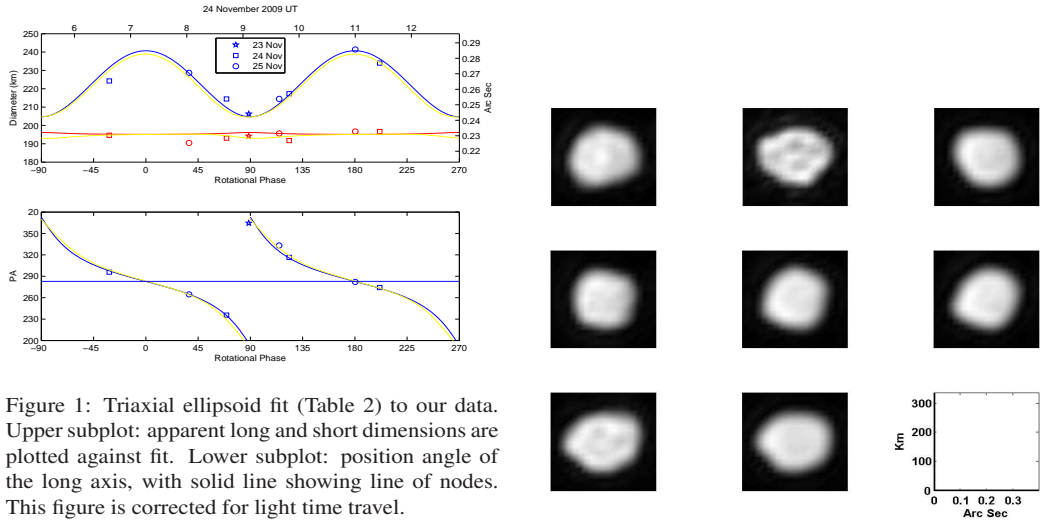


Figure 1: Triaxial ellipsoid fit (Table 2) to our data. Upper subplot: apparent long and short dimensions are plotted against fit. Lower subplot: position angle of the long axis, with solid line showing line of nodes. This figure is corrected for light time travel.

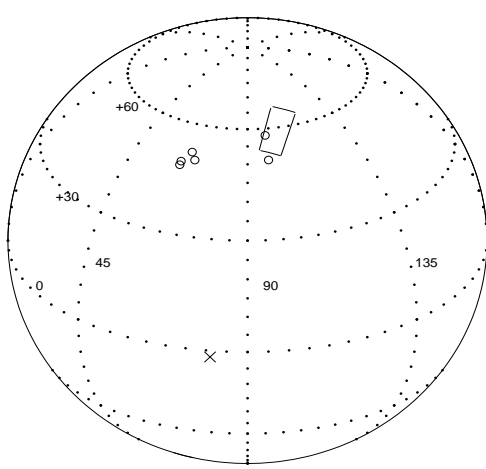


Figure 2: Ecliptic globe with location of Fortuna's rotational poles. The wedge-shaped area is the uncertainty region around our pole, and the X marks the position of Fortuna during our November 2009 observations.

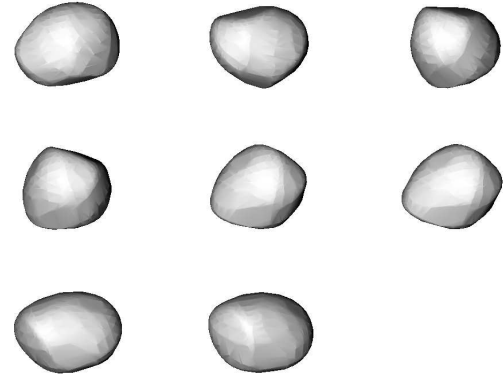


Figure 3: Top: Linearly deconvolved images of Fortuna, November 2009, with scales shown in the blank frame, and with North up and East to the left. The order is the same as in Fig 1. Bottom: Lightcurve inversion model at same rotational phase. The model is projected forward from 1965 with a sidereal period of 7.443224 hr.